PCCP

Cite this: *Phys. Chem. Chem. Phys.*, 2011, **13**, 7773–7782

www.rsc.org/pccp

PAPER

Insights on the mechanism of proton transfer reactions in amino acids†

Fernanda Duarte, Esteban Vöhringer-Martinez and Alejandro Toro-Labbé*

Received 7th October 2010, Accepted 10th February 2011
DOI: 10.1039/c0cp02076a

In the present work, the joint use of the potential energy, the reaction electronic flux profiles and NBO analysis along the intrinsic reaction coordinate within the framework of the reaction force analysis allows us to gain insights into the mechanism of the proton transfer process in amino acids. The reaction was studied in alanine and phenylalanine in the presence of a continuum and with addition of one water molecule acting as a bridge, the results were compared to those of tryptophan. The bridging water molecule stabilizes the zwitterionic form and increases the reaction barriers by a factor of two. This result is interpreted in terms of the energy required to bring the amino acid and the water molecule closer to each other and to promote the proton transfer through the reordering of the electron density. Furthermore, the bridging water molecule induces a concerted asynchronous double proton transfer, where the transfer of the carboxyl hydrogen atom is followed by the second proton transfer to the ammonium group. In addition, a second not intervening water molecule was added, which changes the proton acceptor and donor properties of the reactive water molecule modulating the reaction mechanism. The aforementioned methods allow us to identify the order of the transferred protons and the asynchronicity, thereby, evolving as promising tools to not only characterize but also manipulate reaction mechanisms.

1. Introduction

Amino acids are the basic building blocks of proteins. It is well known that in the gas phase they are predominantly in the canonical (N) form, while in the solid state or aqueous solution the zwitterionic (Z) is the most stable form, which results from favorable solute–solvent electrostatic interactions due to its large dipole moment.[1,2] Basic understanding of the proton transfer (PT) reactions associated with the isomerization process from the neutral amino acid to the corresponding zwitterionic form is essential for many biochemical processes. In the present study, we will employ the potential energy, the reaction electronic flux profiles and the reaction force as a general framework to gain insights on the stability of tautomeric species, the mechanism of the proton transfer and the effect of water in the proton transfer path of alanine, phenylalanine and tryptophan. This information together with the analysis of the evolution of key structural and electronic properties along the reaction coordinate will allow us to elucidate the mechanism of the reaction.

In biological systems, where most of the reactions occur in the solution phase, the solvent effect plays an important role in stabilizing the zwitterionic structure, through electrostatic or/and specific interactions. There is a long-term argument about how many water molecules are necessary to stabilize a zwitterionic amino acid, indicating a strong dependence on the level of theory used in the calculations.[3] Previous studies have shown that at least two water molecules are needed to bind to alanine to give a stable zwitterion cluster in the gas phase.[4–6] Solvent effects also play a crucial role in the mechanism of tautomerization from the neutral to a zwitterionic structure. Two mechanisms for the tautomerization reaction have been proposed: a direct mechanism where the proton transfer occurs directly from the ammonium to the carboxyl group without intervention of solvent molecules, and a water-mediated process, where the proton(s) are transferred through water molecules either in a concerted motion or in a stepwise fashion.[4] The water-mediated tautomerization is an example of the water-mediated multiple proton transfer reactions frequently encountered in biochemical processes.

For the PT reaction in glycine with a discrete water molecule in vacuum the energy barrier of the N→Z tautomerization was calculated to be 9.1 kcal mol^{-1}.[7] Addition of a solvent continuum model reduces the energy barrier to 4 kcal mol^{-1},[7] and replacement of the discrete water molecule with a continuum results in a barrier of 2.4 kcal mol^{-1} at the MP2/6-31+G(d,p) level of theory.[8] For alanine, Ahn *et al.* determined a 0.6 kcal mol^{-1} barrier for a concerted double proton transfer from the neutral to zwitterionic form in the one water complex using water continuum (combining the B3PW91/6-31++G** method and the IEFPCM for

Laboratorio de Química Teórica Computacional (QTC), Facultad de Química, Pontificia Universidad Católica de Chile, Santiago, Chile. E-mail: atola@uc.cl

† Electronic supplementary information (ESI) available. See DOI: 10.1039/c0cp02076a

the water continuum).[5] Rodziewicz and Doltsinis studied microhydration of phenylalanine in vacuum using *ab initio* molecular dynamic simulations and reported the energetically most favorable interconversion path between the neutral and zwitterionic forms to be through a H_2O bridge, with a free energy barrier of 8.3 kcal mol^{-1} for Phe(H_2O) and 3.4 kcal mol^{-1} for Phe(H_2O)$_3$.[9]

Yamabe *et al.*,[10] however, studied the proton-transfer pathways of glycine mediated by n water molecules (n = 0–4) employing a solvent continuum model. They found an energy barrier of 9.93 kcal mol^{-1} for the intramolecular PT and a higher energy barrier for the n-water catalyzed reactions: 11.54 kcal mol^{-1} with n = 1; 14.08 kcal mol^{-1} with n = 2; 10.98 kcal mol^{-1} with n = 3; 12.8 kcal mol^{-1} with n = 4. This is different than in typical reactions, where water-mediated processes have lower barriers than the direct intramolecular transfer. Such phenomena have been postulated in the action of enzymes (*e.g.* carbonic acid anhydrase[11]) as well as in other proton transfer reactions.[2,12–18]

From the above studies one can conclude that the addition of more water molecules does not necessarily lead to a smaller activation barrier. Their concrete position seems much more important and may in some situations catalyze the reaction or change its mechanism. Previous works studied the effect of water molecules either participating in the proton transfer or in coordination with the functional groups of the amino acid. In this study, however, we will focus on the effect of a second water molecule, which is not directly participating in the proton transfer, but acts as a donor or acceptor to the reactive one and may affect the reaction mechanism. In addition, we will compare the PT reaction of tryptophan in our previous study[19] to alanine (Ala) and phenylalanine (Phe). Thereby, we want to address the influence of the amino acid side chain on the proton transfer process in solution, analyze the role played by the solvent in the PT reaction and characterize the physical nature of energy barriers. The latter goal will be achieved by making use of the partition of the activation energy provided by the reaction force analysis.

2. Theoretical background

For any chemical process, the potential energy $E(\xi)$ of the system along the intrinsic reaction coordinate ξ has an associated reaction force $F(\xi)$, defined by:[20]

$$F(\xi) = -\frac{\mathrm{d}E}{\mathrm{d}\xi} \tag{1}$$

For any elementary step, the reaction force profile has a minimum and a maximum at the inflection points of $E(\xi)$, located at ξ_1 and ξ_2. This pattern allows three regions to be defined for a one-step reaction, namely, reactant, transition state, and product, with well-established tendencies as evidenced in ref. 21–24. The reactant region ($\xi_R \leq \xi \leq \xi_1$) involves preparation of reactants to chemical transformation and is dominated by structural arrangements; this step of the reaction requires an amount of work $W_1 = -\int_{\xi_R}^{\xi_1} F(\xi)\mathrm{d}\xi$. The transition state region ($\xi_1 < \xi < \xi_2$) is governed by the transition from activated reactants at ξ_1 to activated products at ξ_2 involving bond breaking/forming processes accompanied by strong fluctuations in some electronic properties. The work that is necessary to reach the TS from ξ_1 is $W_2 = -\int_{\xi_1}^{\xi_{TS}} F(\xi)\mathrm{d}\xi$. Finally the *product* region ($\xi_2 \leq \xi \leq \xi_P$) is mainly dominated by the relaxation process toward the equilibrium geometry of the product.

Within the above scheme the energy barrier, $\Delta E^{\neq}$, can be written as the sum of two contributions $\Delta E^{\neq} = [E(\xi_{TS}) - E(\xi_R)] = W_1 + W_2$. This partitioning proved to be valuable for elucidating the solvent and catalyst effects on specific reactions, *i.e.* whether these effects are primarily structural or electronic.[23,25] For the forthcoming analysis, we also define: $W_3 = -\int_{\xi_{TS}}^{\xi_2} F(\xi)\mathrm{d}\xi$ and $W_4 = -\int_{\xi_2}^{\xi_P} F(\xi)\mathrm{d}\xi$ such that the reaction energy is in turn partitioned as: $\Delta E^{\circ} = W_1 + W_2 + W_3 + W_4$.

2.1 Chemical potential and reaction electronic flux

Within the framework of DFT, the chemical potential for an N-particle system with total energy E and external potential $\upsilon(\boldsymbol{r})$ is defined as follows:[26,27]

$$\mu = \left(\frac{\partial E}{\partial N}\right)_{\upsilon(\boldsymbol{r})} = -\chi \tag{2}$$

where χ is the electronegativity. The use of the finite difference approximation leads to the following working expressions in terms of the first ionization potential, I, and electron affinity, A, respectively:[26, 27]

$$\mu \cong -\tfrac{1}{2}(I + A) \tag{3}$$

The variation of μ along the reaction pathway leads to $\mu(\xi)$. The reaction electronic flux (REF) is defined as the negative of the chemical potential gradient:[28]

$$J(\xi) = -\left(\frac{\mathrm{d}\mu}{\mathrm{d}\xi}\right) \tag{4}$$

$J(\xi)$ describes the electronic activity that is taking place along the reaction coordinate.[29,30] In analogy with thermodynamics concepts, the changes of the chemical potential along the reaction coordinate can be interpreted as describing the spontaneity of the process, so that taking into consideration the sign of $J(\xi)$, positive values of REF will be associated to spontaneous changes in the electronic density and negative values of REF will be related with non spontaneous electronic reordering.

3. Computational methods

All the structures have been fully optimized using the Becke-3 for exchange[31] and Lee–Yang–Parr for correlation[32–34] (B3LYP) functional with the standard 6-31G** basis set. The minimum energy path in going from reactants to products was calculated through the intrinsic reaction coordinate procedure (IRC = ξ)[35,36] using a step size of 0.01 amu$^{1/2}$bohr. Frequency calculations on reactants, transition states, and products were performed to obtain the reported free energies and zero-point energies and to confirm the nature of the corresponding critical point along the reaction path. Using the geometries obtained from the IRC procedure, molecular properties were determined through single point calculations

at the same level of theory. Calculations in solution were performed with the polarizable continuum model (PCM)[37] as implemented in the Gaussian 03 package,[38] where the liquid is represented with a continuum characterized by a dielectric constant of 78.39 for water. The default cavity was modified by adding individual spheres to hydrogen atoms involved directly in the proton transfer (using the keyword SPHEREONH).[38] The extra spheres were necessary to match the isosurface of the electron density in reactants and products (see ESI†) and to keep the hydrogen atoms inside the cavity in the transition states. Since a mixed discrete–continuum model has been already shown to be reliable enough to explain the specific and bulk effects of the solvent on proton transfer reactions,[2,12] we will also use a B3LYP + explicit water + PCM strategy to characterize the water-mediated reactions. The natural bond orbital[39] analysis was also carried out to obtain the Wiberg bond index along the reaction coordinate and to evaluate the direction and magnitude of the donor–acceptor interactions. Reactants, transition state, and products were also optimized at the MP2/6-31G(d,p) level for comparison. All calculations were carried out using the Gaussian 03 program.[38]

4. Results and discussion

4.1 Energetic parameters and potential barriers

Fig. 1 shows the reactions under study: reactions **R1** and **R2** are the intramolecular proton transfer process and reactions **R4** and **R5** are the water-mediated process in alanine and phenylalanine respectively. The potential energy profiles along the intrinsic reaction coordinate for these reactions are displayed in Fig. 2. The IRC calculation did not always converge to the reference structures shown in Fig. 1, but the energy differences from the last IRC point to the optimized reactant or product structure were very small, lower than 1 kcal mol^{-1}. In such cases the last structure of the IRC calculation was fully optimized always converging to the reference structure shown in Fig. 1. The profiles have the classical form of an elementary step, indicating that for the water-mediated proton transfer the mechanism of these processes is a concerted double proton transfer *via* the binding water molecule. Although in proton transfer reactions tunneling and the quantum nature of the proton donor and acceptor atoms may play a role,[40,41] the narrowness of the potential energy surfaces shown in Fig. 1 suggests that tunneling contribution would be small and therefore these effects will not be discussed in the present work.

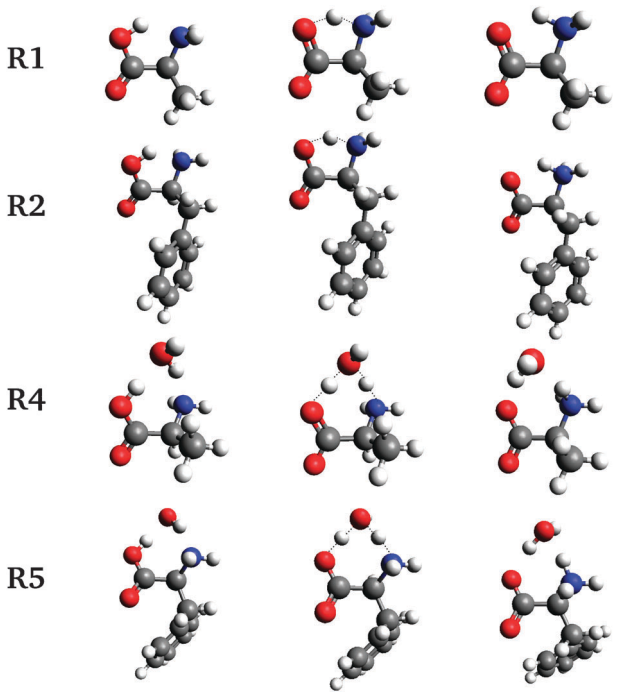

Fig. 1 Optimized structures for the neutral, transition state and zwitterionic form of alanine (**R1** and **R4**) and phenylalanine (**R2** and **R5**). Not shown here is reaction **R3** and **R6** corresponding to tryptophan which is studied in detail in ref. 19.

To initiate this study, the reaction energies (ΔE°) and energy barriers ($\Delta E^{\neq}$) for reactions **R1** and **R4** were also determined using the MP2/6-31G(d,p) method in order to compare different levels of theory. The results are displayed in Table 1 where values from our previous study on tryptophan[19] were also included as **R3** and **R6**, respectively. Energies obtained with the B3LYP method are in good agreement with the MP2 results—the energy barrier differs only by 1 kcal mol^{-1} from the MP2 energies (see Table 1)—in agreement with previous studies.[5,9] Therefore, it can be concluded that the B3LYP/6-31G(d,p) level is suitable to study the title reactions with a good compromise between accuracy and computational cost.

The reaction energies and energy barriers for all reactions considered in this paper are summarized in Table 2. Intramolecular PT reactions are all endoenergetic with similar ΔE° values. It is remarkable that the reaction energies associated with these reactions are about two times those of water-mediated processes. This result emphasizes the key role of the water molecule in stabilizing the zwitterionic structure through specific interactions, which cannot be described only with the continuum model. Also the energetic barrier of the PT process is affected when a discrete water molecule is introduced, $\Delta E^{\neq}$ values in **R4–R7** are about two times those of the intramolecular process; comparison with glycine systems shows the same trend.[7,42]

To account for thermal contributions the reaction and activation free energies of all reactions were calculated within the harmonic approximation (see Table 2). It can be observed that the reaction energies are in agreement with the obtained free energies, whereas the activation free energies are 1–3 kcal mol^{-1} smaller than the activation potential energies. To establish the origin of the observed difference the potential energy values were corrected with the zero-point energy (ZPE) (see Table 2). The obtained values match the activation free energies disclosing the origin of the observed difference between the potential and free energy in the zero-point energy correction. This difference can be rationalized from frequencies in the reactant becoming imaginary ones in the transition state.

4.2 Reaction force profile

Reaction force profiles are comparatively presented in Fig. 3. The critical points at ξ_1 and ξ_2 (dashed vertical lines in the reaction force profiles) define the reaction regions, allowing the energetic barrier decomposition in terms of the work invested in each region (Table 3). The shape of the reaction

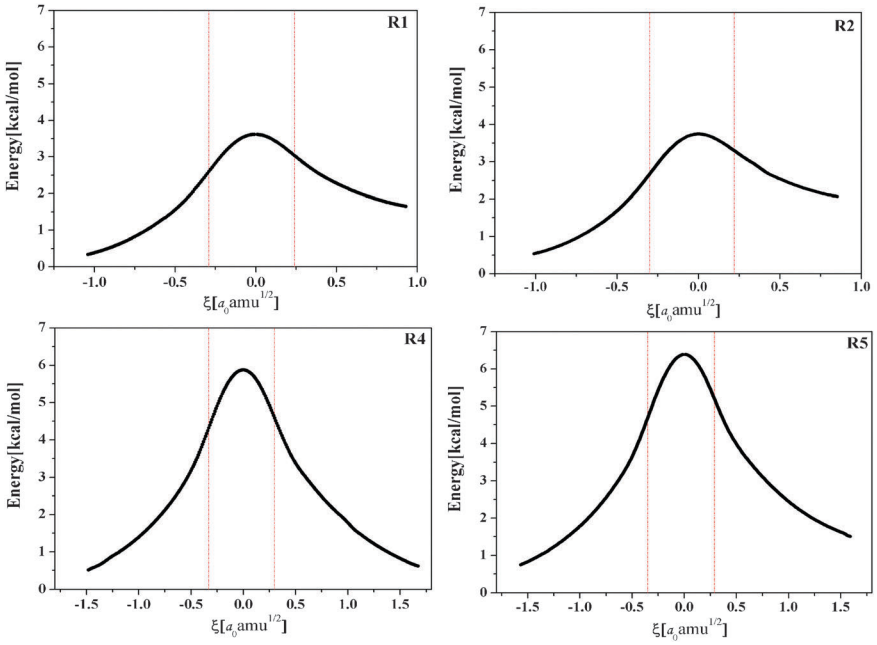

Fig. 2 Energy profile for the intramolecular and water-mediated proton transfer reactions in alanine **R1** and **R4** and phenylalanine **R2** and **R5**, respectively.

Table 1 Reaction energy (ΔE°) and energy barriers ($\Delta E^{\neq}$) of the PT reactions computed at the B3LYP and MP2 levels of theory with the 6-31G(d,p) basis set. All values are in kcal mol^{-1}

Reaction		ΔE°		$\Delta E^{\neq}$	
		DFT	MP2	DFT	MP2
R1	AlaPCM	1.5	0.6	3.6	3.6
R3	TryPCM	1.5	−0.7	3.8	3.7
R4	Ala(H_2O)PCM	−0.6	−2.0	5.9	6.9
R6	Try(H_2O)PCM	−0.8	−2.6	5.7	6.7

Table 2 Reaction and activation energies including the ZPE correction and free energies for the PT reactions computed at the B3LYP/6-31G(d,p) level of theory. All values are in kcal mol^{-1}

Reaction		ΔE°	ΔG°	ΔE°_{ZPE}	$\Delta E^{\neq}$	$\Delta G^{\neq}$	$\Delta E^{\neq}_{ZPE}$
R1	AlaPCM	1.5	1.6	1.7	3.6	1.6	1.4
R2	PhePCM	1.8	1.1	1.9	3.7	1.5	1.5
R3	TryPCM	1.5	1.7	1.8	3.8	1.6	1.6
R4	Ala(H_2O)PCM	−0.6	−0.4	0.0	5.9	2.8	2.2
R5	Phe(H_2O)PCM	0.9	0.3	1.3	6.4	2.5	2.6
R6	Try(H_2O)PCM	−0.8	−0.9	−0.2	5.7	2.5	2.0
R7A	Ala(H_2O)$_2$PCM	−0.7	−0.6	−0.2	5.4	2.7	2.0
R7B	Ala(H_2O)$_2$PCM	−0.6	−0.3	0.1	5.2	2.7	2.1

force profile for the intramolecular and the water-mediated proton transfers do not depend on the nature of the amino acid. The amplitude, however, is smaller in the intramolecular process with respect to the water-mediated one and the relaxation part of the reaction force is less deep and wider than the activation part, in accordance with the fact that the intramolecular process is more endothermic than the water-mediated one.

An initial slope analysis of the reaction force profile shows the evolution of the forces opposing the preparation step. In the water-mediated processes $F(\xi)$ decreases relatively slowly and almost linearly until $\xi = -0.6$, then a rapid decrease sets in until ξ_1, the minimum of $F(\xi)$, denoting a change in the nature of these forces. First, they are mostly related to structural changes, in which the main feature is the approximation of the water molecule to the functional groups of the amino acid (see ESI† where it can be observed that the donor–acceptor distances between the amino acid and water change only in the reactant and product region, indicating that these are mainly structurally active regions). Then, once it reaches $\xi = -0.6$, the breaking/forming bond processes become activated and the proton transfer process is the driving force. This is different from the intramolecular processes, where the first linear decrease in the reaction force is assigned to the approximation between the donor and acceptor functional groups.[18,21]

The reaction works $\{W_1, W_2, W_3, W_4\}$ representing the amount of work involved at each step along ξ are quoted in Table 3 together with the $\{\xi_1, \xi_2\}$ values defining the length of the transition state regions. In previous investigations we showed that the first step of an elementary process is mostly associated with the structural reorganization of the reactants to achieve an activated reactant configuration, reached at ξ_1, while W_2 is largely characterized by reordering in the electronic cloud.[21–24] In those studies we also showed that the effects of external agents upon activation processes are primarily in the initial regions, W_1, where it facilitates the structural changes[18,23,24] thus diminishing the activation energy.

In the present situation however, the water molecule actually increases the energy barrier. It is observed that both W_1 and W_2 values for the water-mediated process are higher than those for the intramolecular one. In the intramolecular process, **R1** for example, the first step of the reaction to reach the minimum of the force requires $W_1 = 2.6$ kcal mol^{-1} which

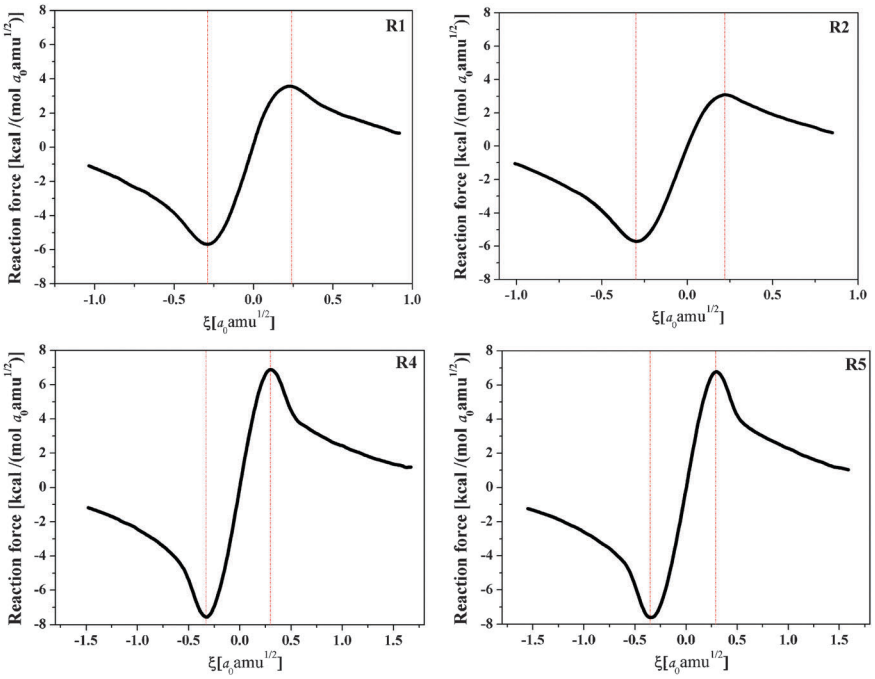

Fig. 3 Reaction force profile for the intramolecular and water-mediated proton transfer reactions in alanine, **R1** and **R4**, and phenylalanine, **R2** and **R5**, respectively.

Table 3 Reaction energy, energy barriers, position of the extreme points of the reaction force $\{\xi_1, \xi_2\}$ and the reaction works of the processes computed at the B3LYP level of theory with the 6-31G(d,p) basis set. Energies and reaction works are given in kcal mol^{-1}; ξ values are given in $a_0$amu$^{1/2}$

Reaction		ΔE°	$\Delta E^{\neq}$	ξ_1	ξ_2	W_1	W_2	W_3	W_4
R1	AlaPCM	1.5	3.6	−0.3	0.2	2.6	1.0	−0.6	−1.5
R2	PhePCM	1.8	3.7	−0.3	0.2	2.7	1.0	−0.5	−1.4
R3[a]	TryPCM	1.5	3.8	−0.3	0.2	2.7	1.1	−0.6	−1.7
R4	Ala(H_2O)PCM	−0.6	5.9	−0.3	0.3	4.3	1.6	−1.3	−5.2
R5	Phe(H_2O)PCM	0.9	6.4	−0.4	0.3	4.8	1.6	−1.2	−4.3
R6[a]	Try(H_2O)PCM	−0.8	5.7	−0.3	0.3	4.3	1.4	−1.3	−5.2
R7A	Ala$(H_2O)_2$PCM	−0.7	5.4	−0.3	0.3	4.0	1.4	−1.3	−4.8
R7B	Ala$(H_2O)_2$PCM	−0.6	5.2	−0.5	0.4	3.3	1.9	−1.2	−4.6

[a] Values from ref. 19.

is the work necessary to approximate the donor and acceptor to each other. The reaction work W_1 is larger than W_2 (1.0 kcal mol^{-1}), which is required to achieve the activation step of the proton transfer. Thus, 72% of the activation barrier principally, but not exclusively, involves structural rearrangement. In the water-mediated process (**R4**) both W_1 and W_2 increase equally by a factor of 1.6, indicating that additional energy is necessary, first to bring the amino acid and the water molecule closer to each other, but also to promote the proton transfer through the reordering of the electron density.

Previous studies in other intramolecular proton transfer processes, where a strained four-member ring conformation has to be reached in order to start the transfer, have shown that addition of a water molecule reduces the energy barrier.[17,18] The energy reduction was observed in nucleic acid bases[17] and in the thioformic acid system[18,21] for example, in which a H_2O molecule leads to a less strained six-member ring at the transition state instead of a four-member ring formed in the intramolecular proton transfer process. But, in this case **R1** has already a less strained intramolecular H-bond—a five-member ring geometry (see Fig. 1)—where the amount of deformation needed to reach the activated reactant structure is comparatively smaller than the referenced proton transfer processes. The participation of a water molecule in the present reactions **R4–R6** necessarily implies an initial reorientation to adopt the right conformation to act as a bridge in the proton transfer, thus involving an additional structural work which is absent in **R1–R3**.

Once the TS is reached, the energy required from the TS to ξ_2, W_3, also increases in the water-mediated processes, by a factor of about 2 with respect to the intramolecular process. The total transition state energy $W_2 + |W_3|$ increases by a factor of about two suggesting an increase of the electronic activity in the transition state region, this will be confirmed with the REF analysis in Section 4.4. Finally, W_4 increases by a factor of three, which explains most of the changes observed in the reaction energy and, in combination with the increase in W_3, the stabilization conferred by the presence of a water molecule to the zwitterionic structure, which is responsible for the high-energy barrier of the reverse reaction in the water-mediated processes.

The nature of the amino acid side chain (methyl, Toulol, 2-methylindole) has practically no effect on the energy barrier. The detailed reaction force analysis shows that the components of the energy barrier, W_1 and W_2, are comparable suggesting that the energetic issue is practically localized within the reactive part of the system and involves the atoms situated at the vicinity of the transferred proton.

4.3 Bond order

The Wiberg bond orders along the reaction coordinate reveal no dependence on the amino acid side chain. The major

changes in the bond orders occur for all reactions within the TS region confirming that it is in this region where the most part of the electronic activity takes place. To gain more insights into the change of the electronic density along the reaction coordinate, we have calculated the derivative of bond orders with respect to the reaction coordinate for the transferred hydrogen and the donor or acceptor atoms (Fig. 4). A negative sign in the derivative indicates bond weakening or dissociation, while a positive sign accounts for bond formation or strengthening.[30]

In the intramolecular processes, the charge transfer taking place during the dissociation of bond O–H and the formation of bond H–N occurs simultaneously: both derivative of the Wiberg bond indices reach their maximum at the TS region. Notice that while those bonds are dissociated and formed, respectively, electronic reordering also takes place in the O═C–O moiety. Both C–O bonds reorganize their electronic density in order to compensate the additional charge due to the migration of the proton. In the water-mediated process, the proton transfer occurs in a concerted but asynchronous way: at the reaction force minimum the first proton transfer takes place between the oxygen of the carboxyl group and the water molecule in combination with the electronic reordering at the O═C–O moiety. Once these derivatives reach their maximum change, the second proton transfer is activated, reaching its maximum at the reaction force maximum.

In the water-mediated process, the asynchronicity of the proton transfer leads to a transition state where the water molecule has three coordinated hydrogen atoms, representing a H_3O^+ hydronium-cation like structure. This is reflected in the shorter hydrogen bond distance of $O_w\cdots H$ bonds (1.19 Å) in comparison to the N$\cdots$H and COO$\cdots$H bonds (1.32 Å and 1.26 Å respectively), as well as in the partial increased positive charge of +0.5 for this complex entering the transition state region. The stability of this species at the transition state and its influence over the mechanism will be analyzed in the last section.

4.4 Reaction electronic flux

In the previous analysis, we have seen that the participation of a water molecule has a strong influence over the energy and mechanism in the PT reaction, whereas for different side chains a smaller influence was observed. In order to explore in depth these aspects the chemical potential $\mu(\xi)$ and electronic flux $J(\xi)$ profiles, calculated from eqn (3) and (4), are analyzed. The electronic flux $J(\xi)$ for the reactions under study is displayed in Fig. 5. As a general feature it can be observed that the electronic activity initiates at the reactant region and the REF profile exhibits in most cases a broad negative peak, which is characteristic of a non-spontaneous electronic activity.

In the intramolecular process **R1** the REF minimum is centered in the transition state, while in **R4** it is shifted to the minimum of the force, with an almost zero flux regimen during the first part of the reactant region (from reactant to $\xi = -0.7$). The energy required at this point in **R4**, which matched the end of the linear decrease of the reaction force, is 1.8 kcal mol^{-1} while in **R1** it is only 0.8 kcal mol^{-1} (from reactant to $\xi = -0.8$). These results confirm the fact that a lower structural work is needed in **R1** to bring the donor and acceptor close to each other to begin the PT process. In contrast, for **R4** the structural rearrangements, identified as the approximation of the water molecule to the functional groups of the amino acid, lead to higher W_1 values. Comparison with the bond order derivative profiles of Fig. 4 suggests

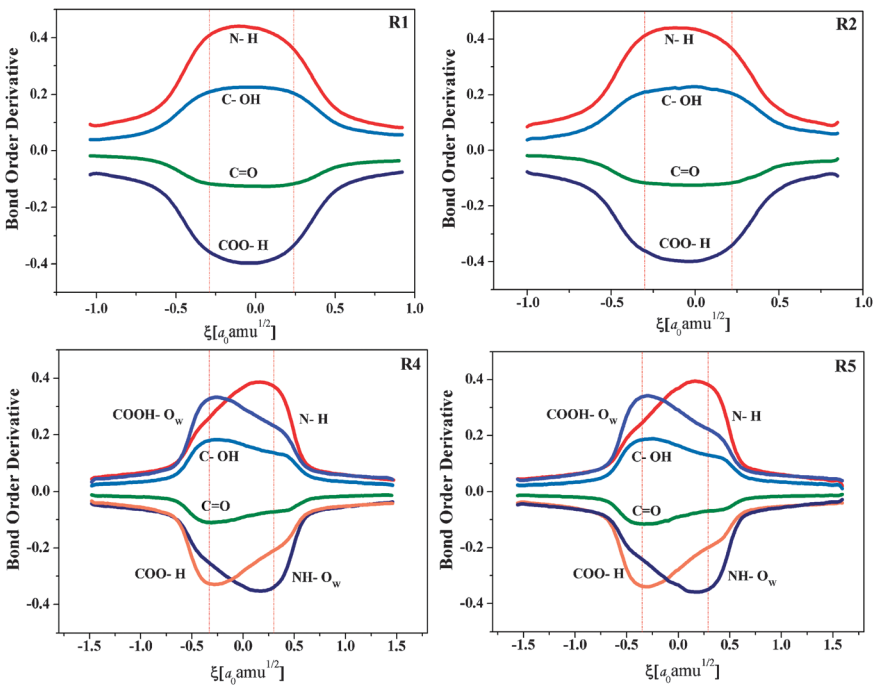

Fig. 4 Bond order derivatives for the bonds being formed and broken in the proton transfer reactions of alanine, **R1** and **R4**, and phenylalanine, **R2** and **R5**, respectively.

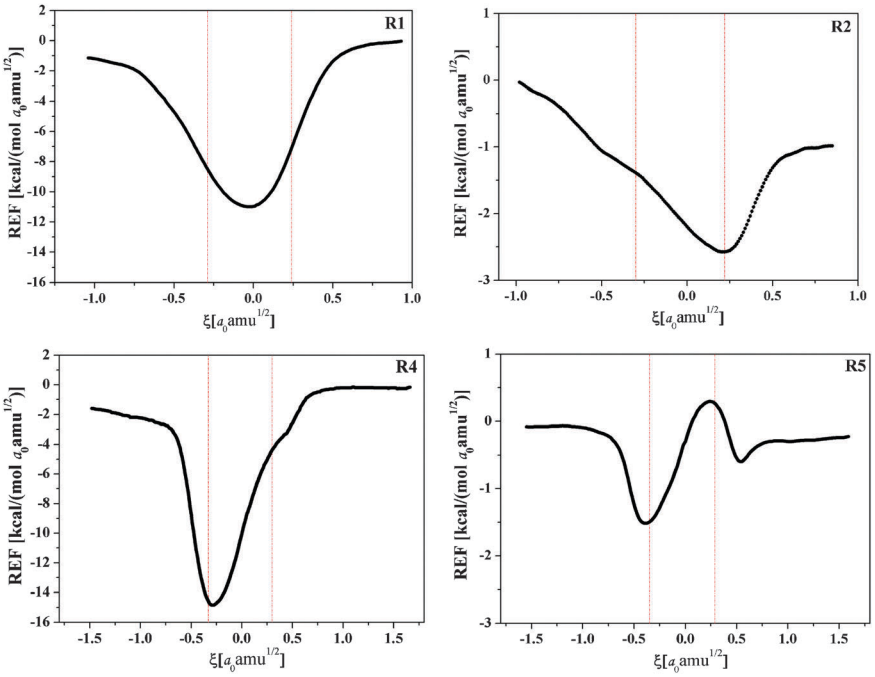

Fig. 5 Profile of the reaction electronic flux for the intramolecular and water-mediated proton transfer reactions in alanine, **R1** and **R4**, and phenylalanine, **R2** and **R5**, respectively.

that the maximum electronic activity (maximum REF) is associated with reordering in the O═C–O moiety. In **R1** the maximum electronic activity is observed at the transition state region, where the electronic reordering in the O═C–O moiety takes place at the same time as when the proton transfer process occurs. In **R4** this reordering occurs earlier, at the reaction force minimum, coupled to the first proton transfer between the oxygen atoms, which correlate with the maximum REF.

Comparing aromatic side chains, as present in phenylalanine (**R2**, **R5**) and tryptophan (ref. 19), with alanine it can be noted that they reveal smaller electronic fluxes. The frontier orbitals of these systems are localized on the aromatic substituents and the large distance to the reactivity centers (NH_3^+ and COO^-) seems to attenuate the REF thus suggesting that its magnitude might be related to the distance of the frontier orbitals to the reactive region of the system. In **R2** the reaction electronic flux decreases monotonically until reaching its minimum value at ξ_2 following the pattern already encountered in **R1**, although the marked asymmetry of the profile should be again attributed to effects of the frontier orbitals on the aromatic ring. For the water-mediated processes, it can be observed that until the transition state they present similar REF profiles: both **R4** and **R5** reach a minimum at ξ_1, where the first proton transfer in the O–H–O moiety is activated, as has been seen before from the bond order analysis. After reaching the transition state a different pattern is observed which in **R5** is most related to changes in the aromatic ring.

4.5 The effect of a second water molecule

As it has been mentioned above, the participation of one water molecule in the proton transfer process leads to a transition state where the water molecule has three coordinated hydrogen atoms, which can be understood from the mentioned distances in section 4.3. This coordination is similar to the one present in H_3O^+-ion. This cation, besides the $(H_5O_2)^+$ and $(H_9O_4)^+$ ions, which are the so-called Zundel[43] and Eigen[44] forms of the cations, respectively, has been the topic of extensive research, since it plays a crucial role in the proton transfer mechanism in neat liquid water.[45,46] It has been proposed that the addition of a second water molecule to the H_3O^+-ion stabilizes the ion forming the Zundel ion.[47,48]

To analyze the possible stabilization of the obtained transition states, a second water molecule was added as a hydrogen donor and as a hydrogen acceptor to **R4**. The respective structures are shown in Fig. 6. In structure **R7A** the second H_2O molecule is positioned over the water oxygen atom acting as a proton donor while in **R7B** it is located right below the other water molecule acting as a proton acceptor, representing a Zundel-cation like structure.

In **R7A** the energy barrier is reduced by 0.5 kcal mol^{-1} and matches the same reaction energy of **R4** (Table 3). The reaction works W_1 and W_4, which are more related to structural rearrangements, are little affected compared to **R4**, while W_2 and W_3 corresponding to electronic changes remain unaffected. The main difference to **R4** is reflected in the reaction mechanism. The second water molecule induces first the transfer of the proton on the water molecule to the amino-group, which represents the reverse order observed in **R4**, while the proton of the carboxyl group is passed at the maximum of the reaction force after reaching the transition state (see Fig. 6). The added water molecule acting as a donor reduces the electron density through the H-bond on the reactive water molecule involved in the proton transfer. This reduction is accompanied with a decreased electronegativity of its oxygen

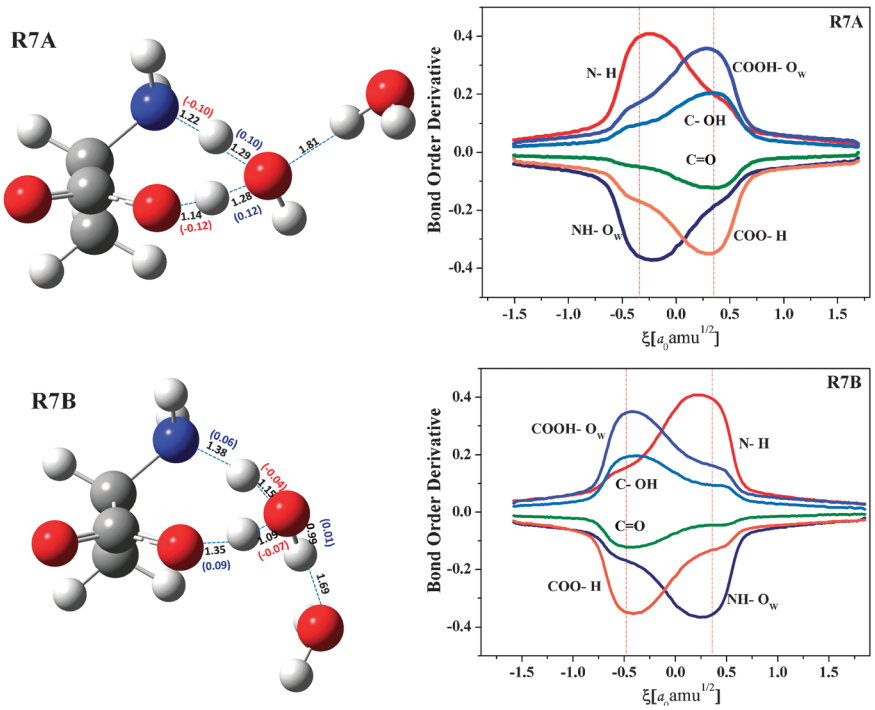

Fig. 6 Transition state structure and bond order derivatives for the systems **R7A** and **R7B**. Values in parentheses show the differences with respect to the bond distances for **R4**.

atom, transforming it into a better proton donor with respect to the nitrogen atom and a worse proton acceptor with respect to the oxygen atom of the carboxyl group. This change in the nature of the water oxygen atom is also observed in the reduced distances with respect to the transition state structure of **R4** between the nitrogen atom and the proton from the water molecule (1.22 Å) as well as in the COO–H distance (see Fig. 6).

In **R7B**, where the H_3O^+-ion is expected to be more stabilized by forming the Zundel-cation, the energy barrier decreases by 0.7 kcal mol^{-1}. Here, the reaction works present the same changes as in **R7A**, although more pronounced. The order of the transferred hydrogens is preserved with respect to **R4**, whereas the absolute value of minimum and the maximum of the reaction force increases leading to a larger transition state region, and therefore an earlier proton transfer of the carboxyl group and a later transfer to the amino group along the reaction coordinate. This is also shown in the bond derivatives, where the respective extrema are more separated. The added water molecule, therefore, transforms the oxygen water molecule in a better acceptor, which is reflected in shorter distances towards the two transferred protons.

This change in the nature of the water oxygen atom over the mechanism was also analyzed with the NBO analysis. The NBO theory describes the formation of a AH$\cdots$B hydrogen bond as the charge transferred from the lone pair n_B of the proton acceptor to the vacant antibonding orbital σ^*_{AH} of the proton donor. The $n_B \rightarrow \sigma^*_{AH}$ delocalization leads to energy lowering that can be quantified by the second order perturbation theory, where the second order perturbation $E^{(2)}_{n_B \rightarrow \sigma^*_{AH}}$ values can be used to estimate the relative strength of hydrogen bonds.

In **R4** two strongest intermolecular interactions are found between nO_w and the σ^* COO–H orbital and between nN and σ^* O_w–H. These interactions cause elongation of the respective X–H bond by increasing the population of its antibonding orbital and, thus, promote the proton transfer process. From the $E^{(2)}_{n_B \rightarrow \sigma^*_{AH}}$ values (see Table 4) it can be concluded that the proton involved in the strengthened hydrogen bond is the one which is transferred first in the direction from the carboxyl group to the water molecule ($E^{(2)}_{n_B \rightarrow \sigma^*_{AH}} = 39.57$ kcal mol^{-1}), in agreement with the order obtained from the bond order derivatives profiles in **R4**.

When a second water molecule is added, acting as a proton donor (**R7A**), the strength of COOH$\cdots$$O_w$ hydrogen bond decreases with respect to the O_wH$\cdots$N hydrogen bond. In this case, due to the intermolecular interactions created between O_w and the O–H of the second water molecule, the electron donor (proton acceptor) ability of the oxygen O_w is reduced in the COOH$\cdots$$O_w$ hydrogen bond ($E^{(2)}_{i \rightarrow j^*} = 31.40$ kcal mol^{-1}), leading to a stronger interaction between the nitrogen lone

Table 4 Summary of the NBO analysis for reactant structures

Reaction	Donor (n_B)	Acceptor (σ^*_{AH})	$E^{(2)}_{n_B \rightarrow \sigma^*_{AH}}$ / kcal mol^{-1}
R4	$LP_{(1)}$ N	BD* O_w–H	30.38
	$LP_{(2)}$ O_w	BD* COO–H	39.57
R7A	$LP_{(1)}$ N	BD* O_{w1}–H	36.94
	$LP_{(2)}$ O_{w1}	BD* COO–H	31.40
	$LP_{(2)}$ O_{w1}	BD* O_{w2}–H	13.27
R7B	$LP_{(1)}$ N	BD* O_{w1}–H	27.26
	$LP_{(2)}$ O_{w1}	BD* COO–H	45.05
	$LP_{(2)}$ O_{w2}	BD* O_{w1}–H	22.57

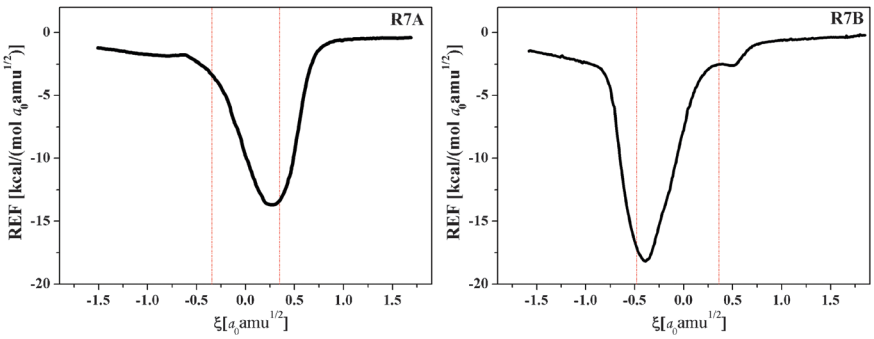

Fig. 7 Profiles of the reaction electronic flux for the water-mediated proton transfer reactions **R7A** and **R7B**.

pair and the σ*O_w–H orbital ($E^{(2)}_{i\rightarrow j^*} = 36.94$ kcal mol^{-1}). Thus, during the proton transfer it is this proton which is transferred first. In **R7B**, where the second water molecule acts as a proton acceptor, a stronger interaction is found in COOH···O_w, thus favoring an earlier proton transfer process ($E^{(2)}_{n_B\rightarrow\sigma^*_{AH}} = 45.05$ kcal mol^{-1}).

It can also be noted that in **R7B** the work W_1 is reduced by 1 kcal mol^{-1} compared to **R4**. This lower value, which is mainly associated to structural rearrangement needed to start the process, is in line with the higher $E^{(2)}_{n_B\rightarrow\sigma^*_{AH}}$ value of the COOH···O_W hydrogen bond in this system. The stronger hydrogen bond in **R7B** at the reactant structure implies that a lower structural reorganization will be necessary to bring the donor and acceptor atoms close to each other to begin the PT process, thus making it more favorable.

In terms of the REF, the addition of a second water molecule leads to a different pattern depending on the character of the second water (see Fig. 7). In **R7A**, when it acts as a proton donor, the REF minimum is shifted from the reaction force minimum to the maximum. Thus, confirming that the REF is mostly associated with reordering in the O═C–O moiety due to the proton transfer from the COOH group to water.

5. Conclusions

A complementary approach based on the reaction force framework has been presented to investigate the intramolecular and water-mediated proton transfer mechanism in amino acids using a solvent continuum model. In addition, the effect of a not intervening water molecule acting as a donor or acceptor with respect to the bridging water molecule has been studied.

The results show that the bridging water molecule stabilizes the zwitterionic form and increases the reaction barriers by a factor of two in all studied systems with a marginal influence of the amino acid side chain (methyl, Toulol, 2-methylindole). About 70% of the activation barrier involves structural rearrangement.

The water-mediated processes correspond to a concerted, though asynchronous, motion of the two protons toward the respective acceptor atoms: the hydrogen atom of the carboxyl group leads the transfer while the hydrogen atom of the bridging water to the ammonium group is transferred later. The NBO analysis has provided a detailed description of the order of the transferred protons and the asynchronicity of the processes. Comparison of these results with the reaction electronic flux profiles suggests that the maximum electronic activity is driven by the electronic reordering in the O═C–O moiety, while the amplitude depends on the nature of the side chain. Aromatic side chains, where the frontier orbitals are not located on the reactive atoms, present smaller fluxes than alanine.

Further, a second water molecule acting as a donor or acceptor with respect to the bridging reactive one reduces in both cases the energy barrier. This not intervening water molecule varies the donor and acceptor character of the reactive one which changes the order of the transferred protons or modulates the earlier or later character of the transfer. The approach presented here, where different theoretical tools merge to provide a complete and consistent picture of proton transfer reactions, illustrates how a water molecule can modulate the mechanism of a chemical reaction.

This work was supported by Fondecyt through project No. 1090460. F.D. wishes to thank CONICYT for a Doctoral and Apoyo de Tesis fellowship and L'OREAL-UNESCO for the *for Women in Science 2009* award. E. V.-M. thanks the Alexander von Humboldt Foundation and the Bundesministerium für Bildung und Forschung for financial support.

References

1 L. Gontrani, B. Mennucci and J. Tomasi, *J. Mol. Struct. (THEOCHEM)*, 2000, **500**, 113.
2 C. Adamo, M. Cossi and V. Barone, *J. Comput. Chem.*, 1997, **18**, 1993.
3 J. H. Jensen and M. S. Gordon, *J. Am. Chem. Soc.*, 1995, **117**, 8159.
4 S.-W. Park, D.-S. Ahn and S. Lee, *Chem. Phys. Lett.*, 2003, **371**, 74.
5 D.-S. Ahn, S.-W. Park, I.-S. Jeon, M.-K. Lee, N.-H. Kim, Y.-H. Han and S. Lee, *J. Phys. Chem. B*, 2003, **107**, 14109.
6 J. M. Mullin and M. S. Gordon, *J. Phys. Chem. B*, 2009, **113**, 8657.
7 B. Balta and V. Aviyente, *J. Comput. Chem.*, 2004, **25**, 690.
8 F. R. Tortonda, J. L. Pascual-Ahuir, E. Silla and I. Tuñón, *Chem. Phys. Lett.*, 1996, **260**, 21.
9 P. Rodziewicz and N. L. Doltsinis, *ChemPhysChem*, 2007, **8**, 1959.
10 S. Yamabe, N. Ono and N. Tsuchida, *J. Phys. Chem. A*, 2003, **107**, 7915.
11 D. Silverman and S. Lindslog, *Acc. Chem. Res.*, 1988, **21**, 30.
12 V. Barone and C. Adamo, *J. Phys. Chem.*, 1995, **99**, 15062.
13 J. Gauld, H. Audier, J. Fossey and L. Radom, *J. Am. Chem. Soc.*, 1996, **118**, 6299.
14 J. Gu and J. Leszczynski, *J. Phys. Chem. A*, 1999, **103**, 2744.

15 X.-C. Wang, J. Nichols, M. Feyereisen, M. Gutowski, J. Boatz, A. Haymet and J. Simons, *J. Phys. Chem.*, 1991, **95**, 10419.
16 D. Li and H. Ai, *J. Phys. Chem. B*, 2009, **113**, 11732.
17 Y. Luo, K. Maeda and K. Ohno, *Chem. Phys. Lett.*, 2009, **469**, 57.
18 F. Duarte and A. Toro-Labbé, *Mol. Phys.*, 2010, **108**, 1375.
19 E. Vöhringer-Martinez and A. Toro-Labbé, *J. Comput. Chem.*, 2010, **31**, 2642.
20 A. Toro-Labbé, *J. Phys. Chem. A*, 1999, **103**, 4398.
21 S. Gutiérrez-Oliva, B. Herrera, A. Toro-Labbé and H. Chermette, *J. Phys. Chem. A*, 2005, **109**, 1748.
22 P. Politzer, A. Toro-Labbé, S. Gutiérrez-Oliva, B. Herrera, P. Jaque, M. C. Concha and J. Murray, *J. Chem. Sci.*, 2005, **117**, 467.
23 E. Rincón, P. Jaque and A. Toro-Labbé, *J. Phys. Chem. A*, 2006, **110**, 9478.
24 J. V. Burda, A. Toro-Labbé, S. Gutiérrez-Oliva, J. S. Murray and P. Politzer, *J. Phys. Chem. A*, 2007, **111**, 2455.
25 J. V. Burda, J. S. Murray, A. Toro-Labbé, S. Gutiérrez-Oliva and P. Politzer, *J. Phys. Chem. A*, 2009, **113**, 6500.
26 R. G. Parr and W. Yang, *Density-Functional Theory of Atoms and Molecules*, Oxford Univ. Press, New York, 1989.
27 P. Geerlings, F. D. Proft and W. Langenaeker, *Chem. Rev.*, 2003, **103**, 1793.
28 B. Herrera and A. Toro-Labbé, *J. Phys. Chem. A*, 2007, **111**, 5921.
29 E. Echagaray and A. Toro-Labbé, *J. Phys. Chem. A*, 2008, **112**, 11801.
30 S. Vogt-Geisse and A. Toro-Labbé, *J. Chem. Phys.*, 2009, **130**, 244308.
31 A. Becke, *J. Chem. Phys.*, 1993, **98**, 5648.
32 C. Lee, W. Yang and R. Parr, *Phys. Rev. B*, 1988, **37**, 785.
33 B. Miehlich, A. Savin, H. Stoll and H. Preuss, *Chem. Phys. Lett.*, 1989, **157**, 200.
34 S. Vosko, L. Wilk and M. Nusair, *Can. J. Phys.*, 1980, **58**, 1200.
35 K. Fukui, *Acc. Chem. Res.*, 1981, **14**, 363.
36 C. González and B. Schlegel, *J. Phys. Chem.*, 1990, **94**, 5523.
37 J. Tomasi, B. Mennucci and R. Cammi, *Chem. Rev.*, 2005, **105**, 2999.
38 M. Frisch, *et al.*, , *GAUSSIAN 03, Revision D.02*, Gaussian, Inc., Wallingford, CT, 2003.
39 A. E. Reed, L. A. Curtiss and F. Weinhold, *Chem. Rev.*, 1988, **88**, 899.
40 M. Tuckerman and D. Marx, *Phys. Rev. Lett.*, 2001, **86**, 4946.
41 A. Pérez, M. E. H. H. Tuckerman and O. von Lilienfeld, *J. Am. Chem. Soc.*, 2010, **132**, 11510.
42 B. Balta and V. Aviyente, *J. Comput. Chem.*, 2003, **24**, 1789.
43 G. Zundel and H. Metzger, *Z. Phys. Chem. (Muenchen, Ger.)*, 1968, **58**, 225.
44 M. Eigen and E. Wicke, *J. Phys. Chem.*, 1954, **58**, 702.
45 M. Tuckerman, K. Laasonen, M. Sprik and M. Parrinello, *J. Chem. Phys.*, 1995, **103**, 150.
46 M. E. Tuckerman, D. Marx, M. L. Klein and M. Parrinello, *Science*, 1997, **275**, 817.
47 L. Ojamae, I. Shavitt and S. Singer, *Int. J. Quantum Chem.*, 1995, **56**, 657.
48 R. Parthasarathi and V. Subramanian, *Characterization of Hydrogen Bonding: From van der Waals Interactions to Covalency*, Springer, 2006.

